BULLETIN OF THE EARTHQUAKE
RESEARCH INSTITUTE
Vol. 47 (1969), pp. 831-848

37. *Wave and Mode Separation with Strain Seismographs.*

By Stewart W. SMITH* and Keichi KASAHARA,

Earthquake Research Institute.

(Read June 24, 1969.—Received June 30, 1969.)

Abstract

Three component strain seismograph systems have not previously been fully utilized for separation of SV and SH waves or for separation of spheroidal and toroidal modes of free vibrations. Two new techniques have now been developed for such separation. They are illustrated with an example of free oscillation separation from the 1964 Alaskan earthquake recorded at Nokogiriyama and for separation of plane SV and SH waves, a recent example of a deep earthquake in the Japan Sea recorded at Yahiko is utilized. In the case of wave separation, no prior knowledge of the epicentral location is required. Comparison is made of this technique with that of the rotational strain seismographs of Ozawa and Watanabe. In the case of free oscillation separation, it is necessary to assume the approximate form of the source mechanism in order that the azimuthal order number of the surface harmonics can be specified. The noise level at the Nokogiriyama station was quite high during the Alaskan earthquake, and as a result only a few modes are clearly identifiable. This data can be presented only as an illustration of the technique of mode separation.

Introduction

Considerable effort has gone into data processing techniques and instrument development for separation and identification of the various modes of elastic vibration of the earth and the various types of elastic waves. One of the most attractive means of separating toroidal vibrations and SH waves from all other signals is to calculate the rigid-body rotation associated with the elastic motion, since these types of waves are the only ones for which this quantity is non-zero. Saito (1969) has done this by means of a large array of long-period seismometers. Some including Watanabe (1963), Ozawa (1967), Hagiwara (1958) and a number of others whose work is unpublished have attempted to develop instruments that respond directly to the rotational component of motion. Substantial difficulties exist however, and as a result, such instruments

*) On leave from Seismological Laboratory, California Institute of Technology.

have not gone beyond the experimental stage. In the present work, an alternative approach is taken to enable the separation of wave and mode types by means of a three-axis strain seismograph. Two techniques are presented, one appropriate for short period plane waves and the other for long period free oscillations. Neither of these techniques enables one to determine the rigid body rotation, since this quantity cannot be determined by means of linear strain seismographs. The approach rather is to postulate a model for the signal in terms of the unknown amplitudes of the different constituents, and to use the observed strain field to solve for these unknowns. The direction of arrival for the wave is not required to carry out the process.

The purpose of the mode separation attempted here is to improve the ability to identify modes of free oscillation of the earth in those regions of the spectrum where there is confusion between higher mode spheroidal oscillations and fundamental mode toroidal vibrations, and to determine which modes have been excited in those regions where there is virtual coincidence between spheroidal and toroidal modes. The purpose of the plane wave technique is to aid in the picking of S wave arrival times and to improve the ability to distinguish differing SH and SV velocities which may be caused by anisotropy in the mantle.

Mode Separation

The elastic displacement of a sphere can be conveniently written in terms of the vector spherical harmonics P, B and C as defined by Morse and Feshbach (1953):

for spheroidal modes,

$$\mathbf{U}_S=[U_l(r)\mathbf{P}_{lm}(\theta,\phi)+V_l(r)\mathbf{B}_{lm}(\theta,\phi)]e^{-i\omega_l^S t},$$

and, for toroidal modes, (1)

$$\mathbf{U}_T=[W_l(r)\mathbf{C}_{lm}(\theta,\phi)]e^{-i\omega_l^T t}.$$

Three arbitrary functions of depth $U_l\ (r)$, $V_l\ (r)$, and $W_l\ (r)$ are required, and can be solved for if the elastic structure is specified, and the excitation function is known. We will use the abreviation $U_l\ (a)=U_l$. U_l and V_l go to make up the spheroidal modes of vibration and W_l represents the contribution of toroidal modes. The approach here will be to formulate the problem such that the values of these three functions, evaluated at the surface $r=a$, can be determined experimentally from a single measurement of the strain tensor. As will be pointed out, this cannot be done without some simplifying assumptions. Since the bulk of data on long period oscillations appears to come from individual long-

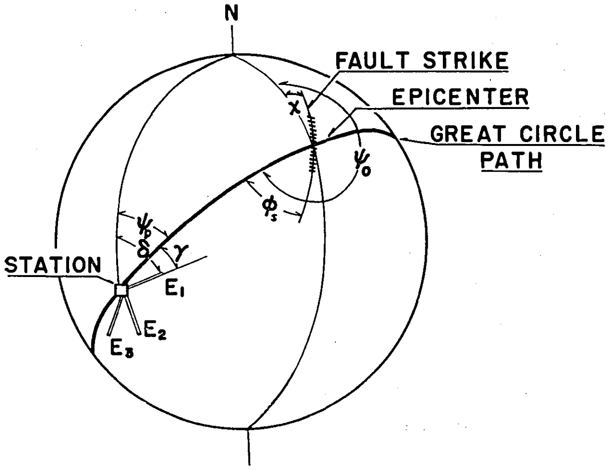

Fig. 1. Geometry and definition of source coordinates. Note that epicentral distance and direction of a nodal line of the source must be known to define source coordinates.

period observatories, and there are not yet enough to make practical those types of analysis that utilize world-wide networks of such data, the present approach seems justified as an attempt to extract more information from a single station than has been heretofor possible. To date, long period pendulums, and 2 axis strain seismographs have been used for analysis. Additional information exists in the third component of a strain seismograph system, that cannot be obtained from a pendulum instrument. Apparently this additional information has not yet been fully utilized in the analysis of propagating waves or elastic vibrations.

The configuration assumed is the most common for strain seismographs, two axes at right angles, and the third at 45°, and in which the reference axis makes an arbitrary angle δ with geographic north. Reference to Fig. (1) shows the definitions and conventions used in defining angles. The first problem is to express the strain tensor in terms of the source coordinates. When this is done, and a simple assumption about the source excitation is made, considerable simplification occurs in the expressions for U_l, V_l, and W_l in terms of the observed extensions along the strain seismograph axes. In what follows, we will assume that for very long periods the earthquake can be viewed as a point source, and that its point force equivalent is a double couple of one of two types. The first type corresponds to a horizontal strike slip motion on a vertical fault plane and only the harmonics with $m=2$ are excited. The other type, corresponds to pure dip slip motion on either a vertical or horizontal fault plane which will excite only harmonics with $m=1$. Experimental evidence from measurement of amplitude patterns of long period surface waves indicates that although this assumption is not strictly true (i. e. propagation effects of the source, and dipping fault planes cause important asymmetries, which call for a distribution of energy over various values of the parameter m), most of the energy in the very long periods can be adequately represented by using only $m=2$, or $m=1$.

Note that all expressions are in terms of the source coordinates, thus θ is the epicentral distance, and ϕ is the azimuth measured from the nodal planes assumed for the source. For great earthquakes for which this process is intended, there is usually ample evidence for such assumptions.

Calculating the strain tensor in terms of the experimentally available extensions El, E2, and E3, we obtain:

$$e_{\theta\phi}=[\mathrm{E1}(\cos 2\gamma+\sin 2\gamma)+\mathrm{E2}(\cos 2\gamma-\sin 2\gamma)-2\mathrm{E3}\cos 2\gamma]D^{-1},$$

$$e_{\theta\theta}-e_{\phi\phi}=[-\mathrm{E1}(\cos 2\gamma+\sin 2\gamma)+\mathrm{E2}(\cos 2\gamma-\sin 2\gamma)+2\mathrm{E3}\cos 2\gamma]D^{-1}, \quad (2)$$

where,

$$D=\cos^3 2\gamma+\frac{1}{2}\sin 2\gamma[1+\cos 2\gamma+\sin 2\gamma].$$

Next, from equation (1), we differentiate to determine the strain tensor in terms of the functions, U, V, and W,

$$\begin{aligned} e_{\theta\theta}&=a_{11}U_l+a_{12}V_l+a_{13}W_l,\\ e_{\phi\phi}&=a_{12}U_l+a_{22}V_l+a_{23}W_l,\\ e_{\theta\phi}&=a_{31}U_l+a_{32}V_l+a_{33}W_l. \end{aligned} \quad (3)$$

At this point we omit the commom exponential term and make the assumption that in range of interest, that is l between 7 and 20, $\omega_l^S\approx\omega_l^T$.

The coefficents a_{ij} are given as follows:

$$a_{11}=a_{21}=a_{31}=X_l^m(\theta,\phi)=P_l^m(\cos\theta)_e^{im\phi},$$

$$a_{12}=\frac{l-m+1}{l+1}(-\cos\theta X_{l+1}^m(\theta,\phi)+\sin\theta X_{l+1}^{m\prime}(\theta,\phi))$$
$$+\frac{l+m}{l}(\cos\theta X_{l-1}^m(\theta,\phi)-\sin X_{l-1}^{m\prime}(\theta,\phi)),$$

$$a_{13}=\frac{im}{l(l+1)}[X_{l+1}^m(\theta,\phi)(l-m+1)(l-1)-(l+2)(l+m)X_{l-1}^m(\theta,\phi)],$$

$$a_{22}=\frac{i}{\sin^2\theta}\{-2A_3\cos\theta X_l^m(\theta,\phi)+A_3\sin\theta X_l^{m\prime}(\theta,\phi)+A_1 m X_{l+1}^m(\theta,\phi)$$
$$-A_2 m X_{l-1}^m(\theta,\phi)\}, \quad (4)$$

$$a_{23}=\frac{1}{\sin^2\theta}\{2A_1\cos\theta X^m_{l+1}(\theta,\phi)-2A_2\cos\theta X^m_{l-1}(\theta,\phi)-A_1\sin\theta X^{m\prime}_{l+1}(\theta,\phi)$$
$$+A_2\sin\theta X^{m\prime}_{l-1}(\theta,\phi)-A_3 m X^m_l(\theta,\phi)\},$$
$$a_{32}=\frac{1}{\sin^2\theta}\{-mA_3X^m_l(\theta,\phi)+A_1\cos\theta X^m_{l+1}(\theta,\phi)-A_2\cos\theta X^m_{l-1}(\theta,\phi)\},$$
$$a_{33}=\frac{im}{l(l+1)\sin^2\theta}\{-(l-1)(l-m+1)X^m_{l+1}(\theta,\phi)+(l+2)(l+m)X^m_{l-1}(\theta,\phi)\},$$

and

$$A_1=\frac{l-m+1}{l+1},$$
$$A_2=\frac{l+m}{l},$$
$$A_3=\frac{m(2l+1)}{l(l+1)}.$$

The notation $X^{m\prime}_l(\theta,\phi)$ indicates differentiation with respect to θ.

Solving equations (3) and (4) for W_l, we obtain the following expression:

$$W_l=\frac{(a_{12}-a_{32})e_{\theta\phi}-a_{22}(e_{\theta\theta}-e_{\phi\phi})}{(a_{12}-a_{32})a_{23}-2a_{22}\,a_{13}}, \tag{5}$$

the experimentally determined values of strain expressed in equation (2) may then be substituted for the final result. Note that it is not necessary to solve independently for U_l and V_l, since the combination $e_{\theta\theta}+e_{\phi\phi}$, which is areal dilatation, already provides a function independent of l, that contains only spheroidal type motion [Smith (1966)].

The above operation are desired for application to the spectrum, however, they may also be used for a narrow band in the time domain. If the signal to noise ratio is good, it is preferable to calculate the numerical complex Fourier transform of the data, and then solve for W_l separately for each l. In case noise is a problem and the power spectrum rather than the Fourier transform must be used, the time series must be transformed using equation (5) before the spectrum is calculated. Since the function W_l is only slowly varying over l in the range $l\geqslant 10$, this can be done for various bands, examining perhaps 4 or 5 modes at a time. This approach seems adequate, since the objective of the technique is to resolve certain specific problems of mode identification in specific frequency bands.

Example of Mode Separation

The authors tested their mode separation technique for the Alaskan earthquake of 1964, utilizing strain seismograms at the Nokogiriyama

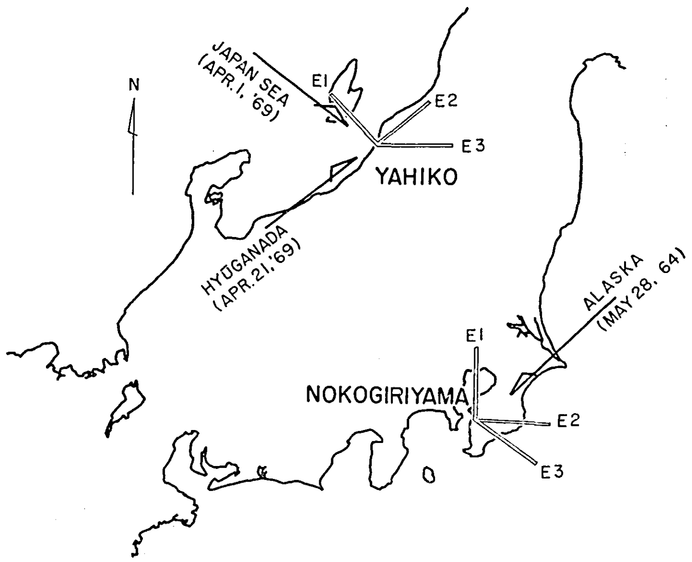

Fig. 2. Relation of direction of wave approach to orientation of strain seismographs for the two examples discussed.

station of E. R. I.. As many other Japanese observatories for crustal movements, the station was equipped with three components of extensometers since its establishment. After several improvements which were applied to them later, the instruments were provided with a function as a three axis strain seismograph system. Fig. 2 shows the station's location and direction of the three axes of the instrument together with the direction of arrival of the seismic signal.

Thus the three components of strains, E1, E2 and E3, due to the earthquake were recorded on charts individually, although the quality of the records was not very good for the present purpose. That is to say, the recording system was designed for tides and secular movements basically, having low paper speed and no DC-cut filters. Relatively high noise level at the station site and frequent adjustment of the recording conditions by the observer during the Alaskan earthquake were another obstacle for the present study. Due to these undesirable conditions, the set of records available for analysis covered a period of 14.4 hours, from 17h30m of May 28 to 07h54m of May 29 (JST).

Practically, the analysis was done in the following procedure:

a) band-pass filtering,
b) mode separation, and,
c) spectral analysis after auto-correlation.

Provided that the records have a good signal-to-noise ratio, an alternative procedure of taking the numerical complex Fourier transform would be preferable. The power spectrum method was decided upon for the present case because the noise level was quite high. As discussed in the previous section, the present technique of mode separation is a non-linear process, basically; so that noise and unnecessary signals should be eliminated at the initial stage in order to reduce contamination of the final result due to these components. The filter was designed so that it may have the pass-band of 8 to 16 min., as the previous analysis [Smith (1966)] seems to promise a high signal-to-noise ratio here.

Next is the principal stage of the present technique, at which mode separation was done on the bases of the foregoing theory. Several parameters were given for this purpose to specify the source conditions and the station's location in the source coordinates [see Fig. 1]. Among them, specifying of l and m would need short remarks. It is already known that the function W in eq. (5) is only slowly varying over l, permitting us to examine 4 or 5 modes in a narrow band simultaneously. Therefore l was fixed at 9 in the present test, which corresponds to the order number at the center of the pass-band. Determination of m would be an interesting problem on source mechanisms in itself. But, in the following, let us simply assume $m=1$, refering to the work by Savage and Hastie (1966). Strictly speaking, excitation by an actual earthquake should be represented, probably, by a combination of several values of m [cf. Ben Menahem (1964)], but the present data is not good enough to permit a detailed discussion.

There is no special remark on the third stage of calculating power spectra for the separated modes, as it refers to the well-established method of spectral analysis. Fig. 3 illustrates the final results thus obtained, in which the spectra of the spheroidal and toroidal components are compared with those of the linear strains recorded in the NS-, EW-, and NW-SE directions, respectively.

It is notable that the energy peaks of the spheroidal and toroidal modes in the 0.08 cpm band are shifted reasonably to one another, corresponding to S_8 and T_8, respectively. Good correlation of their peaks to S_9 and T_{10} is also evident around 0.095 cpm. Agreement of the peaks with prediction is not so clear beyond 0.15 cpm both in the spheroidal and toroidal channels. This region of the spectrum was selected for study because a number of interesting problems in mode identification exist here, as for example the identification of S_{10} and T_{12}. In Fig. 4 we see that S_{10} seems clearly recorded, however T_{12} is not easily discernible. As mentioned earlier, the data for such analysis was not ideal, and it is presented here more as an illustration of the technique. However, it is interesting to note the periods of the modes determined in this way. They are listed below, and compared with values from

Smith (1966).

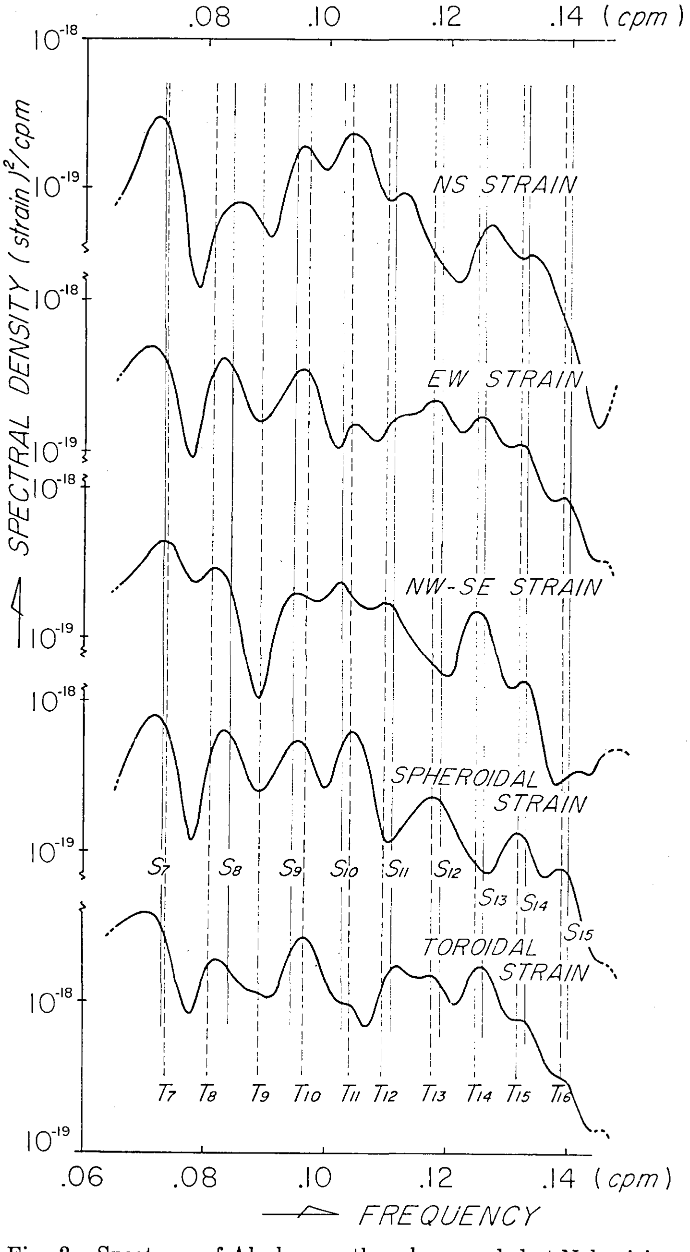

Fig. 3. Spectrum of Alaskan earthquake recorded at Nokogiriyama Upper traces are for individual strain components and lower traces are separated spheroidal and toroidal spectra.

	Nokogiriyama	Isabella
T_8	$12.02^{min.}$	$12.28^{min.}$
T_{10}	10.28	10.33
T_{12}	8.845	8.963
S_8	11.74	11.80
S_9	10.38	10.56
S_{10}	9.500	9.895

The toroidal modes in Fig. 3 have a pronounced difference between even and odd order numbers, with the even order peaks being much more predominant. This effect cannot be a result of the source geometry, or the position of the station. A detailed study has not been made, however it is possible that it is an effect of a propagating or distributed source.

Plane Wave Separation

Data from two horizontal seismometers, or a 2 axis strain seismometer will enable one to determine the ground particle motion associated with a passing seismic wave. From such particle motion, it is often possible to identify wave types and direction of arrival, and also improve the determination of arrival time for various wave types. It is proposed here that a third horizontal component of strain adds new information regarding the direction of approach and mode of propagation of seismic waves, and that this information can further aid in the interpretation of seismograms.

The approach used will be to postulate the form of a wave arrival in terms of unkown amplitudes of longitudinal and transverse wave motion, and direction of approach. In its simplest form, we assume an incident wave consisting of a P or SV wave with amplitude A, and an SH wave with amplitude B incident from an angle θ, which is unspecified. The formulation is for steady state plane harmonic waves, but the intent is to use it on narrow-band filtered seismograms. The strain ellipse produced by this wave will consist of the sum of two strain fields. The contribution of the P or SV wave will have its principal axis at an angle θ to the y axis, and an areal dilation proportional to A, the strain due to the SH contribution will have its principal axis at an angle $\theta \pm 45°$, and an areal dilatation of zero. The technique to be described below is essentially one of trying to determine what possible combinations of such strain fields could give rise to the actual deformation at each instant of time. One cannot do this with conventional pendulum seismographs, or with conventional 2 axis strain seismographs. The third component of strain is essential in defining the instantaneous strain ellipse.

The components of displacement associated with the above wave are

$$u=[A\sin\theta-B\cos\theta]e^{ik(x\sin\theta+y\cos\theta)}\,, \qquad (6)$$
$$v=[A\cos\theta+B\sin\theta]e^{ik(x\sin\theta+y\cos\theta)}\,,$$

and the strains are

$$e_{xx}=A\sin^2\theta-B\sin\theta\cos\theta,$$
$$e_{yy}=A\cos^2\theta+B\sin\theta\cos\theta, \qquad (7)$$
$$e_{xy}=A\sin 2\theta-B\cos 2\theta,$$

omitting the common exponential factor. The amount of areal dilatation, which is the amplitude of the P or SV component is immediately determined from the sum $e_{xx}+e_{yy}=A$.
We can thus write

$$A=e_{xy}\sin 2\theta+(e_{yy}-e_{xx})\cos 2\theta, \qquad (8)$$

$$B=\frac{A\sin 2\theta-e_{xy}}{\cos 2\theta}. \qquad (9)$$

Since A is know, we may solve eq. (8) for $\sin\theta$ and substitute it in the expression for B. Thus from the three independent components of the strain tensor we are able to solve for the three unknowns, that is, the proportions of SV and SH waves, and the direction of approach.

In solving for $\sin\theta$ it was necessary to square both sides of the equation and thus introduce an ambiguity in the sign of the radical in the resulting expression for $\sin\theta$. That this is a physical ambiguity as well as a mathematical one can be seen by considering the response of a strain seismograph to SV and SH wave individually. The response functions for a linear strain seismograph given by Benioff (1935) show a two-lobe pattern ($\cos^2\theta$) for P or SV waves and a four-lobe pattern ($\sin\theta\,\cos\theta$) for SH waves. Thus in the case of an SV wave there is an ambiguity of 180° in determining the direction of arrival, but for an SH wave there is an ambiguity of 90°. As a result, when such wave types are combined, it is not surprising that the resulting ambiguity in direction of airrival is a variable depending on the relative amplitudes of the SV and SH contributions. The behavior of this ambiguity can be investigated quantitatively by plotting both sides of equation (8) as is shown in Fig. 4. In this figure we see that if $A=0$, the case of a pure SH wave, the straight line along the θ axis intersects the curve at two points thus giving two possible solutions for the direction of arrival. In the case of a pure SV wave when $B=0$, we see that $A^2=e_{xy}{}^2+(e_{yy}-e_{xx})^2$ and the straight line intersects the curve at its maximum value thus giving solutions that will be separated by 180°. For combinations of SV

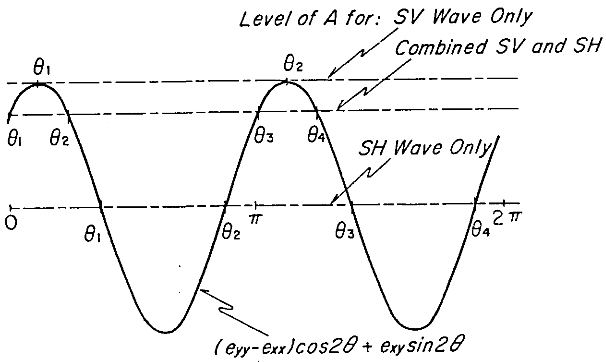

Fig. 4. Solutions to Equation 12 showing possible angles of approach θ_i. Note that in case of a pure SV wave the ambiguity in direction of approach $\theta_2 - \theta_1$ is 180°, and in the case of an SH wave the ambiguity is 90°. Intermediate values are also possible for a combined wave.

and SH waves, as can be seen in Fig. 4, there are in general two possible directions of arrival separated by an amount that is a function of the relative amplitudes A and B. Since the ambiguity cannot be removed without additional information, it is intended to use the process to produce separate SV and SH strain seismograms, as an aid in distinguishing wave arrivals. The ambiguity in direction of arrival can then be removed by looking for consistancy in the directions of arrivals of the stronger phases. In particular, if the P phase can be identified, for which by definition $B=0$, then the direction θ is unambiguously determined from the above process.

Example of Wave Separation

To test the process, a synthetic signal was constructed that corresponded with the direction of approach of an actual earthquake signal to be discussed later. Two cycles of an SV wave were combined with two cycles of an SH wave with an overlap of one cycle as shown in the upper part of Fig. 5. Using this assumed displacement field, the appropriate strains were synthesized for the three component strain seismograph and this data was then sujected to the analysis previously described. The result, shown in the lower two traces of Fig. 5 illustrates that good separation of wave types is possible under these ideal conditions.

A limited amount of data recorded in appropriate form was available from three component strain seismographs. A recent example of a deep earthquake in the Japan Sea recorded at Yahiko Observatory $\Delta=440$ km was chosen to demonstrate the process on actual data. The direction of

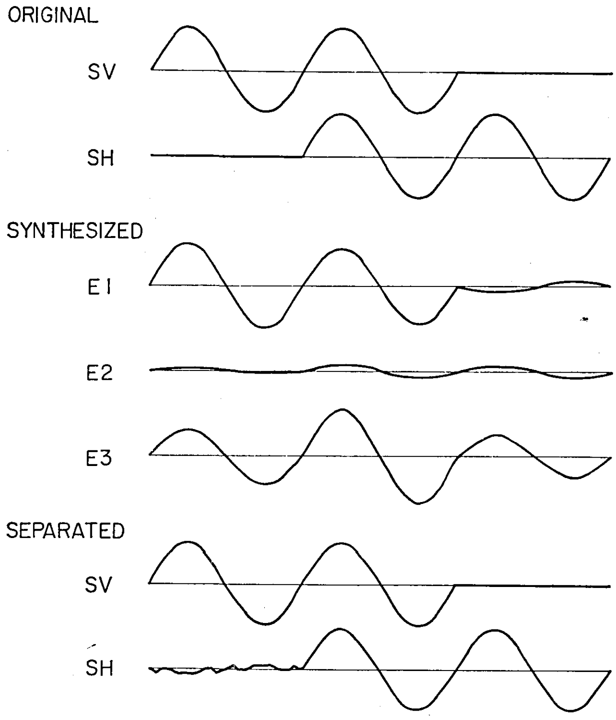

Fig. 5. Synthetic data for test of plane wave separation process. Direction parameters are assumed the same as for actual data shown in Fig. 6.

arrival of this signal with respect to the Yahiko Observatory is illustrated in Fig. 2. The earthquake occurred at 0426 JST, Apr. 1, 1969. The location was approximately 134.0° E., 39.1° N. and the depth was 300 km. The recordings were made through a bandpass filter covering the period range 10 to 3600 seconds. The paper speed was 1.0 mm per second. Time synchronization between channels was approximately $\pm$ 1 second. The original seismograms are shown in the upper traces of Fig. 6. The long-period S phase is indicated on the original traces. On the processed traces we see a fairly clear separation of SV and SH types with the SH arrival approximately 4 seconds earlier than the SV. Considerably more data would have to be collected before commenting on the possible anisotropy for this path, however it is suggestive that the process described here will be appropriate for studies of this type. It is important to note that properties of the wave form other than its time of arrival cannot be obtained from the processed SH seismogram since, because of the nonlinearities involved, the spectrum of the signal is seriously distorted. As in the case of rotational seismographs, the ultimate test of

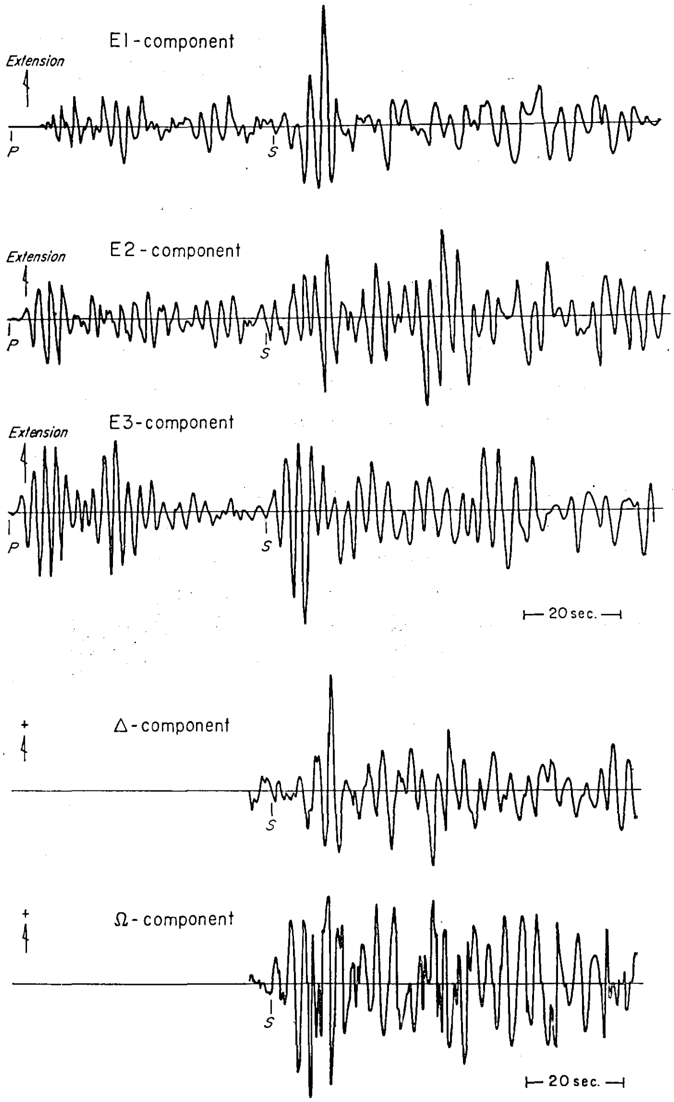

Fig. 6. Seismograms of deep earthquake in Japan Sea recorded at Yahiko. Upper traces are original strain seismograms and lower traces are separated SV and SH seismograms.

the process is to see if the P wave is annihilated on the SH output. Unfortunately, in the only example with which we have been able to work at this time, there is some difficulty in the interpretation of the P wave section of seismograph and it is unsuitable for analysis. On the longitudinal component, the P wave amplitude was unaccountably small. At present we have no adequate explanation of this fact although the difficulty may possibly have been an instrumental or site problem. Subsequent examples for which the entire seismogram can be analyzed will be necessary for a complete evaluation of the proposed process.

Comparison with Rigid Rotation

It is of interest to compare the approach here with the direct measurement of rotation. SH waves or toroidal vibrations are the only wave types that have a non-zero vertical component of the curl of elastic displacement, so that, if this quantity could be measured it would provide a complete separation of these wave types from all others. Furthermore, since rotation is independent of the azimuth of approach of any wave, an instrument that sensed it would have an isotropic response. This would be a great advantage in identifying the onset of the S phase on a seismograms in the presence of the various converted waves and reverberations arriving from different azimuths that often obscure this part of the seismogram. There has been considerable confusion regarding the measurement of rotation associated with SH waves, as a short description of the problem and the approaches used will be given here.

If we consider some finite elastic body, its most general motion

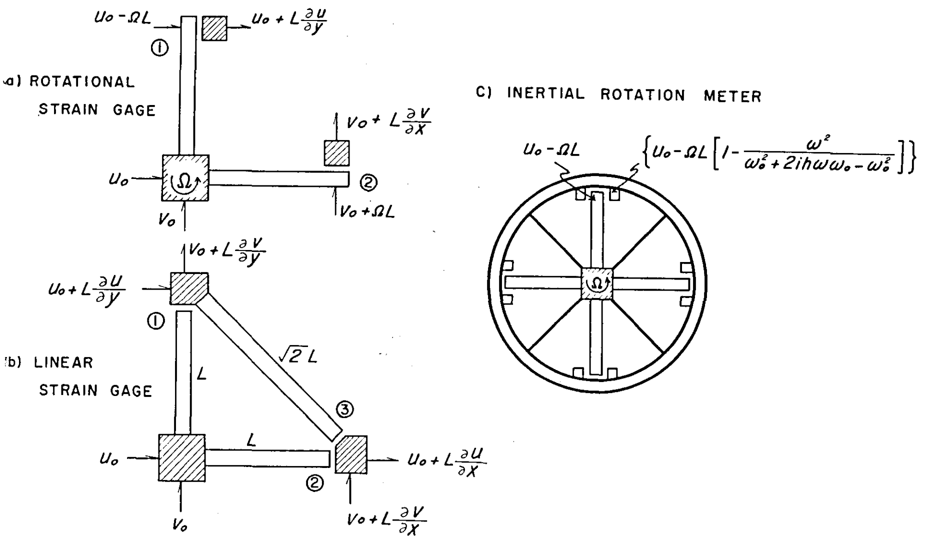

Fig. 7. a) Rotational strain gage. Sum of outputs at transducers (1) and (2) is proportional to rotation Ω at all frequencies.
b) Linear strain gage. Outputs of all transducers are indedendent of rotation Ω.
c) Inertial rotation meter with free period of angular rotation$=\omega_0$ and damping$=$h. For frequencies higher than ω_0 output is proportional to Ω. For frequencies much lower than ω_0 output becomes zero.

consists of a translation, T, a rigid rotation about its center of mass, P, and an elastic distortion S. Therefore,

$$\boldsymbol{D}(x,\ y,\ z)=\boldsymbol{T}+\boldsymbol{P}(x,\ y,\ z)+\boldsymbol{S}(x,\ y,\ z).$$

For the moment, consider both the translation and the rigid rotation to be zero. The elastic distortion S can be represented by a symmetric strain tensor e_{ij} and an antisymmetric rotation Ω_{ij}. The antisymmetric part may also be viewed as a local rigid rotation. To define the distortion of the body, both these components are necessary. Thus, although described as a local rigid rotation, Ω_{ij} corresponds to the twisting deformation of the body, and it can be measured with strain gages such as those described by Watanabe (1963) or Ozawa (1967) as can be seen in Fig. 7a. In this figure which shows the simplest geometry of a rotational strain gage, the sum of the outputs of the transducers at 1 and 2 gives the rotation directly. This is true if the angle between the rigid arms remains 90° and the transducers are perfectly matched. We will return to the question of the angle between the arms later. Looking at Fig. 7b, in which only extensions are measured by the conventional type of strain seismograph that is used in the present study, we see that the output of the three transducers are

$$\mathrm{E1}=\frac{\partial v}{\partial y},\qquad \mathrm{E2}=\frac{\partial u}{\partial x},$$

$$\mathrm{E3}=\frac{1}{2}\left[\frac{\partial u}{\partial x}+\frac{\partial v}{\partial y}-\left(\frac{\partial v}{\partial x}-\frac{\partial u}{\partial y}\right)\right].$$

Here the derivatives $\frac{\partial v}{\partial x}$ and $\frac{\partial u}{\partial y}$ occur only in the combination that we recognize as shear strain. Thus, such an instrument can completely define the elastic strain field, but it cannot give any information about that part of the distortion which we have called local rotation.

Next we consider an inertial rotation meter such as described by Smith et al. (1966) or Hagiwara (1958). In this case, as is shown schematically in Fig. 7c the inertial mass is in the form of an angular ring suspended from a point at the center of a rigid pier. With respect to an inertial reference system. In practice, some type of angular restoring force is provided to give the device stability. It is important to note here that this device differs from the rotational strain gage described above in that it responds to the sum of the local rigid rotation Ω_{ij} and the average rotation P about the center of mass that we initially let be zero, whereas the strain gage sees only the local rotation. As in the case of the rotational strain gage there is also a question about the internal deformation of the instrument itself.

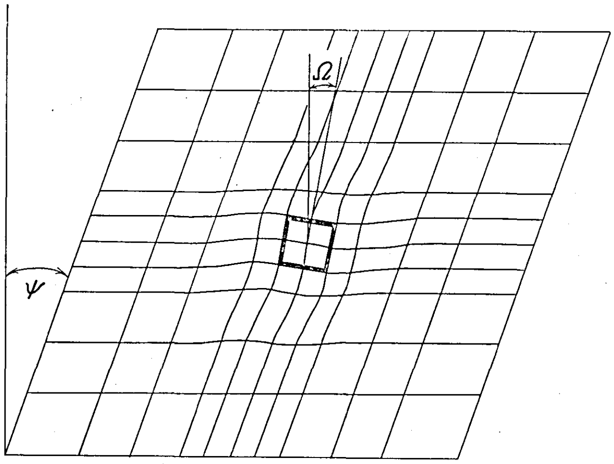

Fig. 8. Deformation in vicinity of rigid instrument base. Lines represent X-Y grid prior to deformation. Angle of shear $\Psi=(\partial u/\partial y+\partial v/\partial x)$. Instrument base rotates an amount $\Omega=1/2(\partial u/\partial y-\partial v/\partial x)$.

Finally, it is possible to determine the velocity of rotation, which is as effective as rotation itself, from a two dimensional array of horizontal pendulum seismographs as was demontrated by Saito (1969). With this approach one needs to determine numerically the values of the derivatives of the elastic displacement function sampled at discrete points by seismic array. Here there is no concern about internal deformation of the instruments, instead one is faced with the problems of precise matching of seismometer characteristics and homogeneity of the earth's crust beneath the array of seismometers. Both these problems seem to be minimized at long periods [Saito (1969)], whereas a similar approach at short periods was unsuccessful [Smith (1966)].

Returning to the question of the internal deformation of instruments used for measuring rotation we can see by considering Fig. 8 that the base of the instrument with respect to which rotation is referred must be attached to the elastic medium, the earth in our case, in at least three points which are not colinear, and that either the instrument base or the earth must be deformed during passage of an elastic wave. If the base deforms, the angle between the arms of either the rotational strainmeter or the inertial rotationmeter will change by an amount proportional to the shear strain. Thus the output of these instruments will become some function of both rotation and shear that depends on the geometry of the instrument and the amount of deformation of the base. For this reason the rigidity of the base and its coupling to the earth become critical considerations for such instruments.

From the above discussion it is clear that substantial problems exist in the realization of seismic instruments for the measurement of rotation. These problems as well as others not mentioned here have so far prevented any widespread use of such instruments, and it is for this reason that we consider in the present paper an alternative procedure for separation of wave types. If there were no noise or other extraneous signals from sources other that the one under consideration, the approach here would give the identical result as the instrumental technique of measuring rotation directly. The result being the amplitude of the SH wave without contamination from P or SV waves. The difference between the techniques becomes apparent if one considers simultaneous arrivals from different directions as is the case with scattered or laterally refracted arrivals. These would not affect the rotation unless they had an SH component, however they may seriously affect the present process. Because it is basically nonlinear, its performance with multiple signals from various azimuths is dependent on the amplitudes of these waves. For this reason, the processes presented here are not intended for the detection of small phases in the presence of much noise. Rather they are intended for phase identification when signal to noise ratios are large and where, as is generally the case for large arrivals, the energy has propagated along a least-time path. Because of these limitations we do not necessarily believe these processes are better for SH separation than the direct instrumental approach, however they do show the possibility of extracting more information from the conventional strain seismograph systems that now exist in may parts of the world.

Acknowledgements

The authors wish to express their appreciation to Professor Takahiro Hagiwara for his role in the establishment of observatories such that at Nokogiriyama, which made this study possible. Our thanks go to the seismologists at Nokogiriyama and Yahiko who furnished the data used here. We also wish to express our appreciation to Professor Yasuo Satô for making avilable various computer programs, and to Miss Masayo Hirai and Miss Akiko Waraya for their technical assistance.

The authors gratefully acknowledge the support of the U. S. Japan Cooperative Science Program under which the U. S. National Science Foundation made possible the visit of one of them (SWS) to the Earthquake Research Institute.

References

BENIOFF, H., 1935, A linear strain seismograph, *Bull. Seism. Soc. Am.*, **25**, 283-309.

SMITH, S. W., 1966, An array process for SH wave, (Abstract), *Trans. Am. Geophys. Un.*, **47**, 171.

SMITH, S., HANSEN, S., and GILMAN, R., April 1966, Horizontal SH wave detector, (Abstract), *Seism. Soc. Am.*.

HAGIWARA, YUKIO, 1958, A rotational seismometer, *Zisin*, [ii], **11**, 141-144.

WATANABE, H., 1963, A rotational strain seismometer, *Jour. Phys. of the Earth*, **11**, No. 2.

OZAWA, IZUO, 1967, Observations of the tidal strains at Osakayama Observatory, Part II, *Disaster Preventions Research Institute Annuals*, No. 10A, 63-75.

SAVAGE, J. and HASTIE, L. M., 1966, Surface deformation associated with dip-slip faulting, *J. Geophys. Res.*, **71**, 4897-4904.

BEN-MENAHEM, A., 1964, Spectral response of an elastic sphere to dipolar point sources, *Bull. Seism. Soc. Am.*, **54**, 1323-1340.

MORSE, P. M., and FESHBACH, H., Methods of theoretical physics, McGraw-Hill Book Co., New York.

---

37. 歪地震計を用いて地震波相または地球振動モードを分離する試み

Seismological Laboratory, C. I. T. Stewart W. SMITH

地震研究所 笠 原 慶 一

三成分歪地震計を用いれば，SV 波と SH 波との分離や地球振動のスフェロイダル・トロイダル両成分の分離ができるはずであるが，従来はあまり関心がもたれなかった．そこで，この目的にかなうよう考えた方法二種類を解析の実例と共に報告することにする．実例に用いられたのは，地球振動のモード分離については鋸山におけるアラスカ地震の記録であり，波相分離については最近日本海中部に発生した深発地震の弥彦における歪地震記録である．なお，前者の場合は地球振動の方位分布に関するオーダー数を指定する必要上，発震機構を知り，または仮定する必要があるけれども，後の波相分離の場合は震央位置が未知であってもかまわない．このようにして試みた結果，特に地球振動の例については原記象の S/N 比がかなり低いにもかかわらず，$S_{8\sim10}$ や $T_{8\sim12}$ の周期について満足すべき値が得られた．

また，波相分離のためには既にいろいろな形式の計器が提案されているが，筆者らの方法とこれら諸型式との原理的な相違についても簡単な考察を加えた．
